

## A STUDY OF THE MIXED MODE I+III LOADING OF A NON-PLANAR CRACK USING INFINITESIMAL DISLOCATIONS

P. N. B. ANONGBA

*U.F.R. Sciences des Structures de la Matière et de Technologie,  
Université de Cocody, 22 BP 582 Abidjan 22,  
Côte d'Ivoire*

(Reçu le 05 Juin 2009, accepté le 10 Décembre 2009)

---

\* Correspondance et tirés à part, e-mail : [anongba@yahoo.fr](mailto:anongba@yahoo.fr)

### ABSTRACT

This paper investigates the mixed mode I+III loading of a non-planar crack that fluctuates about an average fracture  $x_1x_3$  – plane in an infinitely extended isotropic elastic medium. The crack is a continuous array of long non-straight dislocations with infinitesimal Burgers vectors. The dislocations are perpendicular to the  $x_1$  – direction of fracture propagation, have an arbitrary periodic small shape  $\xi = \xi(x_3)$  spreading in the  $x_2x_3$  – plane and their portions may be arbitrarily inclined with respect to the  $x_3$  – direction. The dislocation distribution contains two types of dislocation: dislocations 1 have an edge average character and respond to mode I loading; dislocations 2 have a screw average character and respond to mode III. The displacement and stress fields of two dislocations, with arbitrary shape and average character of edge or screw type, are first given. Expressions for the stress about the crack front and crack extension force  $G$  per unit length of the crack front are also given. Formula for  $\langle G \rangle$ , a spatial average of  $G$ , is provided for one special crack having a segmented front. Conditions under which  $\langle G \rangle$  is maximum conform to experimental measurements of crack-front twist angle versus applied stress.

**Keywords :** *Crack propagation and arrest, energy release rate,  
Dislocations, crack mechanics, energy methods*

### RÉSUMÉ

**Une étude de la sollicitation en mode mixte I+III d'une fissure non plane utilisant des dislocations infinitésimales**

Cet article étudie la sollicitation, en mode mixte I+III, d'une fissure non plane qui fluctue autour d'un plan moyen  $x_1x_3$  dans un milieu élastique

isotrope infiniment étendu. La fissure est une rangée continue de longues dislocations avec des vecteurs de Burgers infinitésimaux. Les dislocations sont perpendiculaires à la direction  $x_1$  de propagation de la fracture, ont une forme arbitraire petite  $\xi = \xi(x_3)$  étalée dans le plan  $x_2x_3$ , et leurs portions peuvent être arbitrairement inclinées par rapport à la direction  $x_3$ . La distribution contient deux types de dislocation : les dislocations de type 1 ont un caractère moyen coin et obéissent au mode I ; les dislocations de type 2 ont un caractère moyen vis et obéissent au mode III. Les champs de déplacement et de contrainte de deux dislocations, avec une forme arbitraire et un caractère moyen coin ou vis, sont d'abord donnés. Des expressions pour la contrainte au niveau du front de fissure et la force d'extension  $G$  de la fissure par unité de longueur du front de fissure sont également données. Une formule d'une moyenne spatiale de  $G$ ,  $\langle G \rangle$ , est établie dans le cas particulier d'une fissure non plane dont le front est segmenté. Des conditions pour lesquelles  $\langle G \rangle$  est maximum sont conformes à des mesures expérimentales d'angles de torsion du front de fissure en fonction de la contrainte appliquée.

**Mots-clés :** *Propagation et arrêt de la fissure , force d'extension de la fissure , dislocations ; mécanique de la rupture , méthodes d'énergies*

## I - INTRODUCTION

The present study belongs to the mechanics of fracture in elastic solids. In what follows, the crack surface is assumed to fluctuate about an average plane because this is the kind of broken surface commonly observed (see below). On the scientific side, the conditions (crack geometries, loading modes ...) under which such cracks develop are not well understood. Of particular interest are methods leading to expressions for the stress about the crack front and crack extension force. The values taken by these quantities, when compared with those corresponding to the planar crack, could then explain the occurrence of non-planar cracks in real materials. With an understanding of fracture development, we can build high performance engines in industry.

In a material containing initially a planar crack, subsequent fracture under mixed mode I+III loading generally occurs on a non-planar surface that fluctuates about the initial crack plane. This observation is derived from numerous experiments performed under various different conditions. The broken surface exhibits the following features, (**Figure 1**) (in glass by

Sommer [1], polymethyl methacrylate (PMMA) by Cooke and Pollard [2], steel by Yates and Miller [3] and Hourlier and Pineau [4], among others):

- For small  $M \equiv \sigma_{23}^a / \sigma_{22}^a \approx 6\%$ , where  $\sigma_{22}^a$  and  $\sigma_{23}^a$  are the applied tension and shear respectively (**Figure 1**), facets  $B$  are almost vertical ( $\phi_B \approx \pi/2$ ) and facets  $A$  horizontal ( $\phi_A \approx 3^\circ$ ); inclination angle  $\phi_A$  of facets  $A$  increases apparently with the extension of the crack (Sommer [1]; see also Lawn [5]).
- $\phi_A$  increases from  $3^\circ$  to  $45^\circ$  approximately as  $M$  increases from zero to infinity [2- 4]. (**Figure 2**), reproduced from Cooke and Pollard [2], shows this trend.

We stress that the shape  $\xi = \xi(x_3)$  of the crack front may differ somewhat from the schematic one shown in **Figure 1**.  $\xi$  may deviate from straight lines for instance. In the present study, we shall present a general treatment by expanding  $\xi$  into a Fourier series.

The study of fracture in mixed mode I+III in solids requires a non-planar crack model that provides expressions for physical quantities pertinent to discuss crack propagation. For this purpose, a relevant quantity is the crack extension force per unit length of the crack front (or energy release rate)  $G$ . Since fracture proceeds through the motion of a macroscopic length of the crack front, it appears necessary to calculate an average  $\langle G \rangle$  and look for a relation between  $M$ ,  $\phi_A$  and  $\phi_B$  that maximizes  $\langle G \rangle$ . This relation may then be confronted with experiments as in **Figure 2**.

A number of theoretical analyses devoted to non-planar cracks have been published. Works by Gao [6], Xu et al. [7] and Movchan et al. [8] refer to perturbation methods where effort is concentrated upon providing stress intensity factor (SIF) formulae that are given to first order in perturbation. SIF expressions are then related to  $G$  by the usual plane strain relation. Under such conditions averaging  $G$ , as performed in the present study in Section 4, simply reduces the result to that of the planar crack; this evidently does not depend on the non-planar crack relevant parameters. Similar works providing first order SIF and involving asymptotic analysis for three-dimensional elasticity problems have also been published (Ball and Larralde [9]; Lazarus et al. [10]). Ball and Larralde [9] were concerned with the stability of mode I cracks. Mixed mode loading was not attainable. Lazarus et al. [10] attempted to explain the increase of  $\phi_A$  with crack length as measured by Sommer [1]. They provided an approximate formula for  $G$  at point  $A$  as defined in **Figure 1** to second order in a parameter, denoted  $d\gamma/d\delta$  by them, that is a measure of the derivative of  $\phi_A$  with respect to crack length. The

obtained relation overestimates actual rotation rates by nearly 3 orders of magnitude [10]. However they obtained a quiet good value of the global rotation rate by a more complex criterion based on the maximization of  $\langle G \rangle$  and SIF expressions but only for three or four point bending experiments. In short, existing theoretical works on non-planar crack growth are seriously limited when applied to mixed mode I+III loading of materials; possible limitations are pointed out in the discussion, Section 5.

We have previously considered a model of non-planar crack under mode I loading that fluctuates about an average plane [11]; the crack has a sinusoidal front perpendicular to the direction of fracture propagation and consists of a continuous distribution of sinusoidal edge dislocations [12]. The stress field of a sinusoidal edge dislocation leads to the stress about the crack front and crack extension force. It is then possible to compare our results with those obtained by other methods and experiments. This approach is maintained in the present work and extended to mixed mode I+III loading; the crack front, instead of being sinusoidal, can now be arbitrary. We provide expressions for stress and crack extension force  $G$  along the crack front, perform an average  $\langle G \rangle$  of  $G$ , establish a relation linking  $M$ ,  $\phi_A$  and  $\phi_B$  that maximizes  $\langle G \rangle$  and finally confront the properties of the model with experiment. The crack consists of a continuous distribution of infinitely long type 1 and 2 dislocations with edge and screw average characters. The dislocations are perpendicular to the  $x_1$  direction of fracture propagation. As for the crack front in **Figure 1**, the shape  $\xi(x_3)$  of the dislocations in the  $x_2x_3$  plane is periodical and fluctuates about an average fracture plane. Elastic fields of the two types of dislocation are given in Sections 2 and 3. We first express the plastic distortion (Section 2.1) and get the associated displacement field using a method developed by Mura [13] as explained in Section 2.2. In Section 4, our crack model and analysis are first presented; then one particular crack with a segmented front is considered. Section 5 confronts the properties of the model with previous works and experiments and concluding remarks are listed in Section 6. A Cartesian system  $x_i$  is used throughout

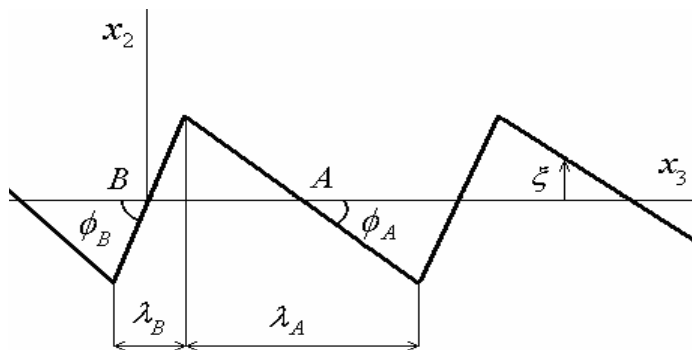


**Figure 1** : Schematic shape of a crack front, in mixed mode I+III loading of a solid, in a plane perpendicular to the  $x_1$  – direction of fracture propagation. The crack fluctuates about the  $x_1x_3$  – plane and consists of planar facets with inclination angle  $\phi_A$  and  $\phi_B$  at point A and B of the average fracture plane, respectively. In this geometry, the crack is subjected to an applied tension  $\sigma_{22}^a$  in the  $x_2$  – direction and shear  $\sigma_{23}^a$  in the  $x_3$  – direction.

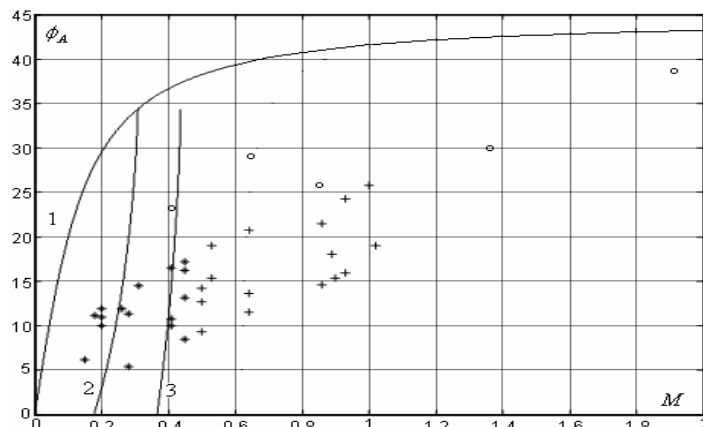


**Figure 2** : Crack-front twist angle  $\phi_A$  (degrees) as a function of the ratio  $M$  (shear/tension) of the applied stresses in polymethyl methacrylate (symbol \* or +) and steel (o) as reproduced from Cooke and Pollard [2]. Curve (1) corresponds to equation (56) in the text; curve (2) and (3) correspond to (52) with  $\phi_B = \pi/2$  and  $\pi/4$  respectively, plots being restricted to  $(M, \phi_A)$  for which  $\langle \tilde{G}_v \rangle$  is maximum and larger than 1.  $\nu = 0.38$  (PMMA).

## II - DISPLACEMENT AND STRESS FIELDS DUE TO A DISLOCATION OF EDGE AVERAGE CHARACTER

### II-1. Plastic distortion

We consider a dislocation at the origin with Burgers vector  $(0, b, 0)$  lying indefinitely in the  $x_3$  direction and spreading in the  $x_2 x_3$  plane in the form of a Fourier series

$$\xi = \sum_n (\xi_n \sin \kappa_n x_3 + \delta_n \cos \kappa_n x_3) . \quad (1)$$

Here  $n$  is a positive integer;  $\kappa_n$  a wave number and  $\xi_n$  and  $\delta_n$  are amplitudes. We assume  $\xi$  to be small and express the plastic distortion  $\beta_{ij}^*(\vec{x})$  to first order in  $\xi$ ; this gives

$$\beta_{12}^*(\vec{x}) = b \delta(x_1) H(x_2) - b \xi \delta(x_1) \delta(x_2) \quad (2)$$

and the other components of  $\beta_{ij}^*(\vec{x})$  are zero, where  $\delta$  and  $H$  are the Dirac delta function and the Heaviside step function, respectively. Here, the first term is due to the straight edge dislocation. The corresponding displacement is known [12]. We shall therefore concentrate on the second term denoted  $\beta_{12}^{*\xi}$ . Its Fourier form may be written as

$$\begin{aligned} \beta_{12}^{*\xi}(\vec{x}) = & \sum_n \sum_{k_{3n}=-\infty}^{\infty} \int_{-\infty}^{\infty} \int_{-\infty}^{\infty} \left( \bar{\beta}_{12}^{*\xi_n}(k_1, k_2, k_{3n}) + \bar{\beta}_{12}^{*\delta_n}(k_1, k_2, k_{3n}) \right) \\ & \times e^{i(k_1 x_1 + k_2 x_2 + k_{3n} \kappa_n x_3)} dk_1 dk_2 \end{aligned} \quad (3)$$

where

$$\times (-b \xi_n \sin \kappa_n x_3 \delta(x_1) \delta(x_2)) dx_1 dx_2 \quad (4)$$

and

$$\begin{aligned} \bar{\beta}_{12}^{*\delta_n}(k_1, k_2, k_{3n}) = & \frac{\kappa_n}{2\pi} \int_{-\pi/\kappa_n}^{\pi/\kappa_n} e^{-ik_{3n} \kappa_n x_3} dx_3 \frac{1}{(2\pi)^2} \int_{-\infty}^{\infty} \int_{-\infty}^{\infty} e^{-i(k_1 x_1 + k_2 x_2)} \\ & \times (-b \delta_n \cos \kappa_n x_3 \delta(x_1) \delta(x_2)) dx_1 dx_2 ; \end{aligned} \quad (5)$$

$k_1$  and  $k_2$  are real and  $k_{3n}$  is a natural number.  $\bar{\beta}_{12}^{*\xi_n}$  and  $\bar{\beta}_{12}^{*\delta_n}$  are non zero only when  $k_{3n} = \pm 1$  and equal to  $\pm ib\xi_n/2(2\pi)^2$  and  $-b\delta_n/2(2\pi)^2$  respectively. The Fourier form of  $\beta_{12}^{*\xi}(\vec{x})$  may be arranged to read

$$\beta_{12}^{*\xi}(\vec{x}) = -\frac{b}{2(2\pi)^2} \sum_n \int_{-\infty}^{\infty} \int_{-\infty}^{\infty} (z_n e^{i(k_1 x_1 + k_2 x_2 - \kappa_n x_3)} + \bar{z}_n e^{i(k_1 x_1 + k_2 x_2 + \kappa_n x_3)}) dk_1 dk_2 \quad (6)$$

where  $z_n = \delta_n + i\xi_n$  and  $\bar{z}_n = \delta_n - i\xi_n$ .

## II-2. Displacement and stress fields

The displacement  $u_m(\vec{x})$  ( $m = 1, 2, 3$ ) due to a plastic distortion of the form  $\beta_{ij}^*(\vec{x}) = \bar{\beta}_{ij}^*(\vec{k}) e^{i\vec{k}\vec{x}}$  where  $\vec{k} = (k_1, k_2, k_3)$  and  $\vec{x} = (x_1, x_2, x_3)$  has been obtained by Mura [13] to be

$$u_m(\vec{x}) = -ik_l c_{klji} L_{mk}(\vec{k}) \bar{\beta}_{ij}^*(\vec{k}) e^{i\vec{k}\vec{x}}. \quad (7)$$

For isotropic material,

$$L_{mk}(\vec{k}) = \frac{\delta_{km}(\lambda + 2\mu)k^2 - k_k k_m(\lambda + \mu)}{\mu(\lambda + 2\mu)k^4} \quad (8)$$

where  $k^2 = k_1^2 + k_2^2 + k_3^2$  and

$$c_{klji} = \lambda\delta_{kl}\delta_{ji} + \mu\delta_{kj}\delta_{li} + \mu\delta_{ki}\delta_{lj}, \quad (9)$$

$\delta_{ij}$  being the Kronecker delta and  $\lambda$  and  $\mu$  are Lamé constants. According to (7),  $u_m(\vec{x}) = -ik_l c_{kl21} L_{mk}(\vec{k}) \bar{\beta}_{12}^*(\vec{k}) e^{i\vec{k}\vec{x}}$  if  $\beta_{12}^*$  is given as  $\bar{\beta}_{12}^*(\vec{k}) e^{i\vec{k}\vec{x}}$ . In the present case however  $\beta_{12}^*$  is given by (6). The linear theory of elasticity allows for the superposition of solutions, so that the corresponding solution may be written as

$$u_m^\xi(\vec{x}) = -\frac{b}{2(2\pi)^2} \sum_n \int_{-\infty}^{\infty} \int_{-\infty}^{\infty} \left( -ik_l c_{kl21} L_{mk}(\vec{k}') z_n e^{i\vec{k}' \cdot \vec{x}} - ik_l c_{kl21} L_{mk}(\vec{k}) \bar{z}_n e^{i\vec{k} \cdot \vec{x}} \right) dk_1 dk_2, \quad (10)$$

in which  $\vec{k}' = (k_1' = k_1, k_2' = k_2, k_3' = -\kappa_n)$  and  $\vec{k} = (k_1, k_2, k_3 = \kappa_n)$ . With (8) and (9), we may arrange (10) to read

$$u_i^\xi(\vec{x}) = \frac{b}{4\pi(1-\nu)} \sum_n (\xi_n \sin \kappa_n x_3 + \delta_n \cos \kappa_n x_3) \left\| (1-2\nu) - x_i \frac{\partial}{\partial x_i} \right\| \times \frac{\partial}{\partial (x_1 \delta_{i2} + x_2 \delta_{i1})} I_n \quad (11)$$

and

$$u_3^\xi(\vec{x}) = -\frac{b}{4\pi(1-\nu)} \sum_n \frac{\partial}{\partial x_3} (\xi_n \sin \kappa_n x_3 + \delta_n \cos \kappa_n x_3) x_2 \frac{\partial}{\partial x_1} I_n, \quad (12)$$

where

$$I_n = \frac{1}{2\pi} \int_{-\infty}^{\infty} \int_{-\infty}^{\infty} \frac{1}{k_1^2 + k_2^2 + \kappa_n^2} e^{i(k_1 x_1 + k_2 x_2)} dk_1 dk_2 = K_0[\kappa_n r], \quad (13)$$

the subscript  $i$  taking the values 1 or 2 in (11); the term in  $\| \cdot \|$  is an operator that acts on the factor with  $I_n$ ;  $r^2 = x_1^2 + x_2^2$ .  $K_n[x]$  is the  $n$ th-order modified Bessel function usually so denoted and  $\delta_{ij}$  is the Kronecker delta. Finally, the total displacement takes the form:

$$u_i(\vec{x}) = u_i^0(\delta_{i1} + \delta_{i2}) + \frac{b}{4\pi(1-\nu)} \sum_n \left\| \delta_{i1} + \delta_{i2} + \delta_{i3} \frac{\partial}{\partial x_3} \right\| A_n \frac{\kappa_n (x_1 \delta_{i2} + x_2 \delta_{i1} + x_1 x_2 \delta_{i3})}{r} \times \left( -\frac{\kappa_n x_i^2 (\delta_{i1} + \delta_{i2})}{r} K_0[\kappa_n r] + \left( (\delta_{i1} + \delta_{i2}) \left( 2\nu - 1 - \frac{2x_i^2}{r^2} \right) + \delta_{i3} \right) K_1[\kappa_n r] \right), \quad (14)$$

subscript  $i = 1, 2$  and  $3$ ;  $A_n = \xi_n \sin \kappa_n x_3 + \delta_n \cos \kappa_n x_3$ ; the term in  $\| \cdot \|$  is an operator that acts on  $A_n$ ;  $\nu$  is Poisson's ratio.  $u_i^0$  is the displacement due to a straight edge dislocation:

$$\begin{aligned}
u_1^0(\vec{x}) &= -\frac{b(2\nu-1)}{8\pi(1-\nu)} \ln(r^2) - \frac{b}{4\pi(1-\nu)} \frac{x_1^2}{r^2}, \\
u_2^0(\vec{x}) &= -\frac{b}{2\pi} \tan^{-1}\left(\frac{x_1}{x_2}\right) - \frac{b}{4\pi(1-\nu)} \frac{x_1 x_2}{r^2}.
\end{aligned} \tag{15}$$

The stress field can be obtained by differentiating the displacement. We find:

$$\begin{aligned}
\sigma_{ii}(\vec{x}) &= \sigma_{ii}^0(\vec{x}) + \frac{Cx_1 x_2}{r^2} \sum_n \kappa_n A_n \left( \kappa_n \left[ -(\delta_{i1} + \delta_{i2}) + \frac{4(x_1^2 \delta_{i1} + x_2^2 \delta_{i2})}{r^2} + 2\nu \delta_{i3} \right] K_0[\kappa_n r] \right. \\
&\quad \left. + \frac{1}{r} \left[ -2(\delta_{i1} + \delta_{i2}) + 4\nu \delta_{i3} + \kappa_n^2 (x_1^2 (\delta_{i1} - \delta_{i3}) + x_2^2 (\delta_{i2} - \delta_{i3})) + \frac{8(x_1^2 \delta_{i1} + x_2^2 \delta_{i2})}{r^2} \right] K_1 \right), \\
\sigma_{12}(\vec{x}) &= \sigma_{12}^0(\vec{x}) + C \sum_n \kappa_n A_n \left( \kappa_n \left[ -\nu + \frac{4x_1^2 x_2^2}{r^4} \right] K_0[\kappa_n r] \right. \\
&\quad \left. + \frac{1}{r} \left[ -1 + \frac{\kappa_n^2 x_1^2 x_2^2}{r^2} + \frac{8x_1^2 x_2^2}{r^4} \right] K_1[\kappa_n r] \right), \\
\sigma_{j3}(\vec{x}) &= C \frac{x_1 \delta_{j2} + x_2 \delta_{j1}}{r} \sum_n \kappa_n \frac{\partial A_n}{\partial x_3} \left( -\frac{\kappa_n (x_1^2 \delta_{j1} + x_2^2 \delta_{j2})}{r} K_0[\kappa_n r] \right. \\
&\quad \left. + \left[ \nu(\delta_{j1} + \delta_{j2}) - \frac{2(x_1^2 \delta_{j1} + x_2^2 \delta_{j2})}{r^2} \right] K_1[\kappa_n r] \right), \tag{16}
\end{aligned}$$

where subscripts  $i$  and  $j$  take the values (1, 2 and 3) and (1 and 2) respectively,  $C = \mu b / 2\pi(1-\nu)$  and  $\sigma_{ij}^0$  is the stress due to the straight edge dislocation:

$$\begin{aligned}
\sigma_{12}^0(\vec{x}) &= C \frac{x_2(x_1^2 - x_2^2)}{r^4}, \\
\sigma_{ii}^0(\vec{x}) &= C \frac{x_1}{r^2} \left( \frac{x_1^2(\delta_{i1} + \delta_{i2}) + x_2^2(-\delta_{i1} + 3\delta_{i2})}{r^2} + 2\nu \delta_{i3} \right), \quad i = 1, 2 \text{ and } 3.
\end{aligned} \tag{17}$$

Note that  $\sigma_{j3}^0(\vec{x}) = 0$  ( $j = 1$  and  $2$ ).

We indicate here a useful observation. From equations (14) and (16), those due to a dislocation with the form  $\xi = \xi_n \sin \kappa_n x_3 + \delta_n \cos \kappa_n x_3$  may be obtained by removing the symbol  $\Sigma$  (in (14) and (16)). Conversely from the knowledge of the elastic fields due to a dislocation with the simple form  $\xi = \xi_n \sin \kappa_n x_3$ , we arrive at those corresponding to a dislocation with the more general form (1), simply by adding  $\Sigma$  to the fields and writing  $\xi_n \sin \kappa_n x_3 + \delta_n \cos \kappa_n x_3$  instead of  $\xi_n \sin \kappa_n x_3$  and  $\kappa_n(\xi_n \cos \kappa_n x_3 - \delta_n \sin \kappa_n x_3)$  instead of  $\kappa_n \xi_n \cos \kappa_n x_3$ .

### III – DISPLACEMENT AND STRESS FIELDS DUE TO A DISLOCATION OF SCREW AVERAGE CHARACTER

We consider a dislocation with Burgers vector  $(0,0,b)$  lying in the  $x_3$  – direction and spreading in the  $x_2 x_3$  – plane in the Fourier series form (1). The only non-zero component of the plastic distortion is written to first order in  $\xi$ :

$$\beta_{13}^*(\vec{x}) = b\delta(x_1)H(x_2) - b\xi\delta(x_1)\delta(x_2) \quad (18)$$

that is identical to (2). Here, the first term is due to the straight screw dislocation. The corresponding displacement is known, see for instance Mura [13]. The Fourier form of the second term is identical to that (6) of  $\beta_{12}^{*\xi}$ . To get the total displacement field, we proceed exactly as for the dislocation of edge average character (Section 2). The result is

$$\begin{aligned} u_i(\vec{x}) = & u_i^0(\vec{x})\delta_{i3} + \frac{b}{4\pi(1-\nu)} \sum_n \left\| \kappa_n x_1 \delta_{i3} + (\delta_{i1} + \delta_{i2}) \frac{\partial}{\partial x_3} \right\| A_n \\ & \times \left( ((1-2\nu)\delta_{i1} + \kappa_n \delta_{i3}) K_0[\kappa_n r] + \frac{\kappa_n x_1 (x_1 \delta_{i1} + x_2 \delta_{i2}) - 2(1-\nu)\delta_{i3}}{r} K_1[\kappa_n r] \right); \quad (19) \end{aligned}$$

$u_3^0$  is the displacement due to a straight screw dislocation [13]:

$$u_3^0(\vec{x}) = \frac{b}{2\pi} \tan^{-1} \left( \frac{x_2}{x_1} \right). \quad (20)$$

The stress field can be obtained by differentiating the displacement. We get:

$$\begin{aligned} \sigma_{ii}(\vec{x}) &= Cx_1 \left( \frac{\delta_{i1} + \delta_{i2}}{r} + \delta_{i3} \right) \sum_n \kappa_n \frac{\partial A_n}{\partial x_3} \left( \kappa_n \left[ -\frac{x_1^2 \delta_{i1} + x_2^2 \delta_{i2}}{r} + \delta_{i3} \right] K_0[\kappa_n r] \right. \\ &\quad \left. + \left[ \frac{(-\delta_{i1} + \delta_{i2})(x_1^2 - x_2^2)}{r^2} - 2\nu \delta_{i2} - \frac{2}{r} \delta_{i3} \right] K_1[\kappa_n r] \right), \\ \sigma_{12}(\vec{x}) &= C \frac{x_2}{r} \sum_n \kappa_n \frac{\partial A_n}{\partial x_3} \left( -\frac{\kappa_n x_1^2}{r} K_0[\kappa_n r] + \left[ \nu - \frac{2x_1^2}{r^2} \right] K_1[\kappa_n r] \right), \\ \sigma_{j3}(\vec{x}) &= \sigma_{j3}^0(\vec{x}) + C \sum_n A_n \frac{\kappa_n}{r} \left( \frac{\kappa_n (x_1^2 + \nu x_2^2) \delta_{j1} + (1-\nu) x_1 x_2 \delta_{j2}}{r} K_0[\kappa_n r] \right. \\ &\quad \left. + \left[ -\kappa_n^2 (x_1^2 \delta_{j1} + x_1 x_2 \delta_{j2}) + \frac{(1-\nu) ((x_1^2 - x_2^2) \delta_{j1} + 2x_1 x_2 \delta_{j2})}{r^2} \right] K_1[\kappa_n r] \right). \end{aligned} \quad (21)$$

$\sigma_{ij}^0$  is the stress due to a straight screw dislocation:

$$\sigma_{i3}^0(\vec{x}) = \frac{\mu b}{2\pi} \left( \frac{x_1 \delta_{i2} - x_2 \delta_{i1}}{r^2} \right), \quad i=1 \text{ and } 2. \quad (22)$$

Note that  $\sigma_{ii}^0(\vec{x}) = 0$  ( $i = 1, 2$  and  $3$ ) and  $\sigma_{12}^0 = 0$ .

## IV - ANALYSIS OF THE NON-PLANAR CRACK

### IV-1. The model

The dislocations with edge (Section 2) and screw (Section 3) average characters are now considered to be continuously distributed over the interval  $x_1 = -a$  to  $a$  (the particular case in which the dislocations have a sinusoidal shape may serve here to illustrate, (Figure 3)). The medium is assumed to be

infinite isotropic and elastic and subjected to uniform applied tension  $\sigma_{22}^a$  and shear  $\sigma_{23}^a$  at infinity. The dislocation distribution function  $D_i(x_1)$  ( $i=1$  for the edges and  $i=2$  for the screws) gives the number of dislocations  $i$  in a small interval  $dx_1$  about  $x_1$  as  $D_i(x_1)dx_1$ . Dislocations 1 and 2 have a Burgers vector  $(0,b,0)$  and  $(0,0,b)$  respectively and to anyone located at  $x_1$  a running point  $P=(x_1, \xi(x_3), x_3)$  ( $\xi$  being given by (1)) and corresponding line sense  $\vec{t}=(1/\sqrt{1+(\partial\xi/\partial x_3)^2}, 0, \partial\xi/\partial x_3, 1)$  are associated. We are concerned with the problem of finding the equilibrium distributions of the dislocations under the combined action of their mutual repulsions and the force exerted on them by  $\sigma_{22}^a$  and  $\sigma_{23}^a$ . We shall derive the equilibrium relations which are given by the condition that each of the infinitesimal dislocations is acted on by zero total force along  $x_1$ . We stress here that the present analysis closely follows previous works representing a crack as a continuous array of dislocations by Bilby et al. [14] and Bilby and Eshelby [15].

Consider a dislocation 1 located at  $x_1$  in **Figure 3**. The force  $dF_1^{(1)}$  in the  $x_1$  direction exerted on it at an arbitrary point  $P$  by the dislocations 1 and 2, located in a small interval  $dx_1$  about  $x_1$ , is obtained from the Peach and Koehler [16] formula to be

$$dF_1^{(1)} = b \sum_{i=1}^2 \left( \sigma_{22}^{(i)} t_3 - \sigma_{23}^{(i)} t_2 \right) D_i(x_1) dx_1 \quad (23)$$

where  $\sigma_{22}^{(i)}$  and  $\sigma_{23}^{(i)}$  ( $i = 1$  and 2) are the stresses due to a dislocation  $i$  at  $x_1$  and  $t_j$  ( $j = 2$  and 3) are the components at  $P$  of the dislocation line sense  $\vec{t}$ . The distribution produces the force

$$F_1^{(1)} = b \sum_{i=1}^2 \int_{-a}^a \left( \sigma_{22}^{(i)} t_3 - \sigma_{23}^{(i)} t_2 \right) D_i(x_1) dx_1 \quad (24)$$

The condition that the total force at  $P$  be zero is evidently

$$\sigma_{22}^a - \sigma_{23}^a t_2 / t_3 + \sum_{i=1}^2 \int_{-a}^a \left( \sigma_{22}^{(i)} - \sigma_{23}^{(i)} t_2 / t_3 \right) D_i(x_1) dx_1 = 0 \quad (25)$$

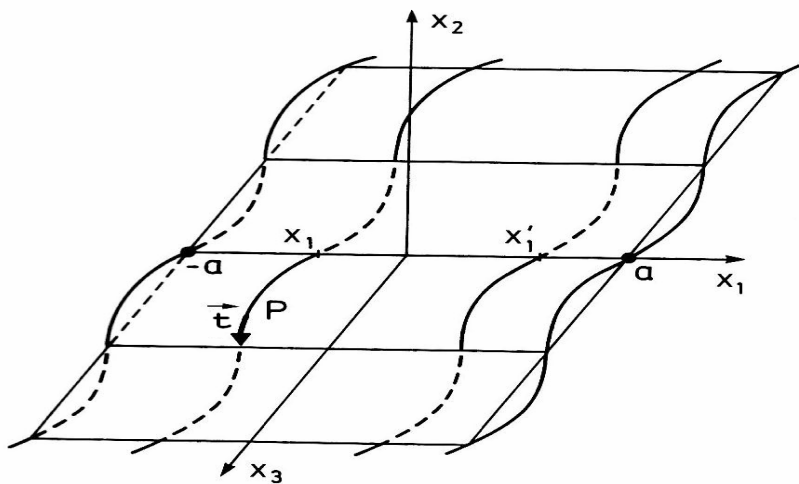


**Figure 3** : A wavy crack with a sinusoidal front, extending from  $x_1 = -a$  to  $a$ , subjected to uniform  $\sigma_{22}^a$  and  $\sigma_{23}^a$  at infinity. The crack fluctuates about a mean plane, which is illustrated, with small amplitude (say roughly of the order of  $1 \mu m$ ).

Similarly the condition that the total force in the  $x_1$  – direction be zero at  $P$  on a dislocation 2 is

$$\sigma_{23}^a + \sum_{i=1}^2 \int_{-a}^a \left( \sigma_{23}^{(i)} - \sigma_{33}^{(i)} t_2 / t_3 \right) D_i(x_1) dx_1 = 0 \quad . \quad (26)$$

(25) and (26) are integral equations that provide the equilibrium distributions  $D_1$  and  $D_2$  of the dislocations. (25) may be arranged in a different form: first an expression for  $\sigma_{23}^a$  is extracted from (26); this formula is then introduced into (25) to obtain a new relation. The pair to solve may be written as

$$\begin{aligned} \sigma_{22}^a + \sum_{i=1}^2 \int_{-a}^a \left( \sigma_{22}^{(i)} - \sigma_{33}^{(i)} (t_2 / t_3)^2 \right) D_i(x_1) dx_1 &= 0 \\ \sigma_{23}^a + \sum_{i=1}^2 \int_{-a}^a \left( \sigma_{23}^{(i)} - \sigma_{33}^{(i)} t_2 / t_3 \right) D_i(x_1) dx_1 &= 0 \quad . \end{aligned} \quad (27)$$

## IV-2. Dislocation distributions

Assume first that the dislocations are straight parallel to the  $x_3$  – direction. We thus have a planar crack in the  $x_1 x_3$  – plane, extending from  $x_1 = -a$  to  $a$ , under mixed mode I+III loading. Under such conditions  $t_2 = 0$ ,  $\sigma_{23}^{(1)} = \sigma_{22}^{(2)} = 0$ ,  $\sigma_{22}^{(1)} = C_1 / x_1 - x_1^*$ ,  $\sigma_{23}^{(2)} = C_2 / x_1 - x_1^*$  (see Sections 2 and 3) where  $C_1 = \mu b / 2\pi(1-\nu)$  and  $C_2 = \mu b / 2\pi$ ; (27) becomes

$$\begin{aligned} \sigma_{22}^a + C_1 \int_{-a}^a \frac{D_1(x_1)}{x_1 - x_1^*} dx_1^* &= 0 \\ \sigma_{23}^a + C_2 \int_{-a}^a \frac{D_2(x_1)}{x_1 - x_1^*} dx_1^* &= 0 \end{aligned} \quad (28)$$

where the Cauchy principal values of the integrals are to be taken. The solution is well known [15]:

$$\begin{aligned} D_1(x_1) &= \frac{\sigma_{22}^a}{\pi C_1} \frac{x_1}{\sqrt{a^2 - x_1^2}} \equiv D_0^{(1)}(x_1) \\ D_2(x_1) &= \frac{\sigma_{23}^a}{\pi C_2} \frac{x_1}{\sqrt{a^2 - x_1^2}} \equiv D_0^{(2)}(x_1) \end{aligned} \quad . \quad (29)$$

$D_0^{(1)}$  corresponds to the distribution of straight edges under pure mode I loading and  $D_0^{(2)}$  to straight screws under pure mode III. The corresponding relative displacements of the crack faces, in the  $x_2$  and  $x_3$  directions, are:

$$\begin{aligned} \phi_0^{(1)}(x_1) &= (\sigma_{22}^a b / \pi C_1) (a^2 - x_1^2)^{1/2}, \\ \phi_0^{(2)}(x_1) &= (\sigma_{23}^a b / \pi C_2) (a^2 - x_1^2)^{1/2}. \end{aligned} \quad (30)$$

Thus it appears that  $D_0^{(i)}$  is unbounded at  $x_1 = \pm a$  and the  $\phi_0^{(i)}$  curve is vertical at these end points.

We now turn to the dislocations with shape Equation (1). To solve (27) we choose for convenience  $P$  on the average fracture plane. This means that  $P = (x_1, 0, x_3^*)$  where  $x_3^*$  satisfies the equation  $\xi(x_3^*) = 0$ . Consequently, with the help of the dislocation stress fields in Section 2 and 3, we may write the various stresses appearing in (27) as

$$\begin{aligned}
\sigma_{22}^{(1)} &= \frac{C_1}{x_1 - x_1^*}, \quad \sigma_{33}^{(1)} = \frac{2\nu C_1}{x_1 - x_1^*}, \quad \sigma_{23}^{(2)} = \frac{C_2}{x_1 - x_1^*}, \\
\sigma_{23}^{(1)}(\vec{x}) &= \nu C_1 \left( \frac{\partial \xi(x_3^*) / \partial x_3}{x_1 - x_1^*} + \sum_n \kappa_n \partial A_n(x_3^*) / \partial x_3 \operatorname{sgn}(x_1 - x_1^*) R_1[\kappa_n |x_1 - x_1^*|] \right), \\
\sigma_{22}^{(2)}(\vec{x}) &= \frac{1-2\nu}{1-\nu} C_2 \left( \frac{\partial \xi(x_3^*) / \partial x_3}{x_1 - x_1^*} + \sum_n \kappa_n \partial A_n(x_3^*) / \partial x_3 R_1[\kappa_n |x_1 - x_1^*|] \right), \\
\sigma_{33}^{(2)}(\vec{x}) &= -\frac{C_2}{1-\nu} \left( \frac{2\partial \xi(x_3^*) / \partial x_3}{x_1 - x_1^*} + \sum_n \kappa_n \partial A_n(x_3^*) / \partial x_3 \right. \\
&\quad \left. \times \left[ -2\operatorname{sgn}(x_1 - x_1^*) R_1[\kappa_n |x_1 - x_1^*|] + \kappa_n |x_1 - x_1^*| K_0[\kappa_n |x_1 - x_1^*|] \right] \right) \quad (31)
\end{aligned}$$

where  $\operatorname{sgn}(x_1 - x_1^*) = |x_1 - x_1^*| / (x_1 - x_1^*)$  and  $R_1[x]$  is the bounded part of the modified Bessel function of first order  $K_1[x]$ :  $K_1[\kappa_n |x_1 - x_1^*|] = 1/\kappa_n |x_1 - x_1^*| + R_1[\kappa_n |x_1 - x_1^*|]$ . (27) becomes

$$\begin{aligned}
&\sigma_{22}^a + C_1 \int_{-a}^a \frac{1-2\nu(\partial \xi(x_3^*) / \partial x_3)^2}{x_1 - x_1^*} D_1(x_1^*) dx_1^* + \frac{C_2}{1-\nu} \int_{-a}^a \left( \frac{\partial \xi(x_3^*) / \partial x_3 (1-2\nu+2(\partial \xi(x_3^*) / \partial x_3)^2)}{x_1 - x_1^*} \right. \\
&\quad \left. + \sum_n \kappa_n \partial A_n(x_3^*) / \partial x_3 f_n(x_1, x_3^*; x_1^*) \right) D_2(x_1^*) dx_1^* = 0 \\
&\sigma_{23}^a + \nu C_1 \int_{-a}^a \left( -\frac{\partial \xi(x_3^*) / \partial x_3}{x_1 - x_1^*} + \sum_n \kappa_n \partial A_n(x_3^*) / \partial x_3 \operatorname{sgn}(x_1 - x_1^*) R_1[\kappa_n |x_1 - x_1^*|] \right) D_1(x_1^*) dx_1^* \\
&\quad + \frac{C_2}{1-\nu} \int_{-a}^a \left( \frac{1-\nu+2(\partial \xi(x_3^*) / \partial x_3)^2}{x_1 - x_1^*} + \sum_n \kappa_n \partial A_n(x_3^*) / \partial x_3 g_n(x_1, x_3^*; x_1^*) \right) D_2(x_1^*) dx_1^* = 0 \quad (32)
\end{aligned}$$

where

$$\begin{aligned}
f_n(x_1, x_3^*; x_1^*) &= (1-2\nu-2(\partial \xi(x_3^*) / \partial x_3)^2 \operatorname{sgn}(x_1 - x_1^*)) R_1[\kappa_n |x_1 - x_1^*|] \\
&\quad + \kappa_n (\partial \xi(x_3^*) / \partial x_3)^2 |x_1 - x_1^*| K_0[\kappa_n |x_1 - x_1^*|], \\
g_n(x_1, x_3^*; x_1^*) &= \partial \xi(x_3^*) / \partial x_3 \left( -2\operatorname{sgn}(x_1 - x_1^*) R_1[\kappa_n |x_1 - x_1^*|] \right. \\
&\quad \left. + \kappa_n |x_1 - x_1^*| K_0[\kappa_n |x_1 - x_1^*|] \right). \quad (33)
\end{aligned}$$

Note that  $f_n$  and  $g_n$  are bounded when  $x_1'$  tends to  $x_1$ . (32) is a system of two integral equations with Cauchy type singular kernels. The numerical resolution of this system with two unknowns  $D_1$  and  $D_2$  may be performed in the same way as for a single equation with one unknown (Anongba [11]; Anongba and Vitek [17]). The solution reads

$$\begin{aligned} D_1(x_1) &= \frac{a\sigma_{22}^a}{C_1} D_0(x_1) \sum_{n=1}^N \alpha_n^{(1)} T_n(x_1/a) \\ D_2(x_1) &= \frac{a\sigma_{23}^a}{C_2} D_0(x_1) \sum_{n=1}^N \alpha_n^{(2)} T_n(x_1/a) \quad , \quad |x_1| < a ; \end{aligned} \quad (34)$$

where  $D_0(x_1) = 1/\pi\sqrt{a^2 - x_1^2}$  is the solution of the homogeneous equation  $\int_{-a}^a (1/x_1 - x_1') D_0(x_1) dx_1' = 0$ ,  $T_n$  are the Chebyshev polynomials of first kind,  $N$  and the coefficients  $\alpha_n^{(i)}$  ( $i=1$  and 2) are obtained numerically using (32) as described by Anongba [11]. Corresponding relative displacements  $\phi_i$  ( $i=1$  and 2) of the faces of the crack, in the  $x_2$  and  $x_3$  directions, are similarly

$$\begin{aligned} \phi_1(x_1) &= \frac{ab\sigma_{22}^a}{\pi C_1} \sum_{n=1}^N \frac{\alpha_n^{(1)} \sin(n \cos^{-1}(x_1/a))}{n} \\ \phi_2(x_1) &= \frac{ab\sigma_{23}^a}{\pi C_2} \sum_{n=1}^N \frac{\alpha_n^{(2)} \sin(n \cos^{-1}(x_1/a))}{n} \quad , \quad |x_1| \leq a . \end{aligned} \quad (35)$$

### IV-3. Stresses about the crack front

When the equilibrium distributions  $D_1$  and  $D_2$  of the dislocations have been found (Section 4.2), the total stress  $\bar{\sigma}_{ij}$  due to the non-planar crack at any point  $(x_1, x_2, x_3)$  is

$$\bar{\sigma}_{ij} = \bar{\sigma}_{ij}^{(1)} + \bar{\sigma}_{ij}^{(2)} \quad (36)$$

where

$$\bar{\sigma}_{ij}^{(n)}(x_1, x_2, x_3) = \sigma_{ij}^{(n)a} + \int_{-a}^a \sigma_{ij}^{(n)}(x_1 - x_1', x_2, x_3) D_n(x_1') dx_1' \quad (n=1 \text{ and } 2); \quad (37)$$

here  $\sigma_{ij}^{(n)}$  ( $n = 1$  or  $2$ ) is the stress field produced by a dislocation at the origin with Burgers vector  $(0, b, 0)$  or  $(0, 0, b)$ .  $\sigma_{ij}^{(n)a}$ , the applied stress, is equal to zero except  $\sigma_{22}^{(1)a} = \sigma_{22}^a$  and  $\sigma_{23}^{(2)a} = \sigma_{23}^a$ . We are interested in stress values in the neighbourhood of the crack front at  $x_1 = a$ . Substituting  $x_1 = a + s$ ,  $0 < s \ll a$ , the stress  $\bar{\sigma}_{ij}$  is given by the following formula:

$$\bar{\sigma}_{ij}(s, x_2, x_3) = \sum_{n=1}^2 \int_{a-\delta a}^a \sigma_{ij}^{(n)}(a + s - x_1', x_2, x_3) D_n(x_1') dx_1' \quad \text{with } \delta a \ll a;$$

this stress expression means that only those dislocations located about the crack front in  $x_1$ -interval  $[a - \delta a, a]$  will contribute significantly to the stress at  $x_1 = a + s$  ahead of the crack tip as  $s$  tends to zero; any other contribution will be negligible for a sufficiently small value of  $s$ . We note that this formula is precise with no place for any other kind of additional stress term. We restrict ourselves to singularities of the type  $s^{-1/2}$  only; this is the singularity that comes into play in the study of planar cracks and gives a well-defined value to the crack extension force. It is sufficient to identify  $\sigma_{ij}^{(n)}$  to the unbounded terms with  $1/(a + s - x_1')$  in the MacLaurin series expansion of  $\sigma_{ij}^{(n)}$  to first order with respect to  $x_2$  (assuming  $x_2$  to be small). Under such conditions the involved integrals are of the type  $\int D_n(x_1')/(a + s - x_1') dx_1'$  which is calculated approximately taking for  $D_n$  the straight edge and screw dislocation distributions corresponding to a planar crack (29). We get

$$\begin{aligned} \bar{\sigma}_{ii}(s, x_2, x_3) = & \left[ \left[ \delta_{i1} + \delta_{i2} + 2\nu\delta_{i3} + \left( \frac{\delta_{i1} - \delta_{i2}}{2} + (1 + \nu)\delta_{i3} \right) x_2 \frac{\partial^2 \xi}{\partial x_3^2} \right] K_I^0 \right. \\ & \left. + \frac{1}{1 - \nu} (-\delta_{i1} + (1 - 2\nu)\delta_{i2} - 2\delta_{i3}) \frac{\partial \xi}{\partial x_3} K_{III}^0 \right] \frac{1}{\sqrt{2\pi} \sqrt{s}}, \end{aligned}$$

$$\bar{\sigma}_{23}(s, x_2, x_3) = \left( \nu \frac{\partial \xi}{\partial x_3} K_I^0 + \left[ 1 + \frac{3-\nu}{2(1-\nu)} x_2 \frac{\partial^2 \xi}{\partial x_3^2} \right] K_{III}^0 \right) \frac{1}{\sqrt{2\pi s}}, \quad \bar{\sigma}_{12} = \bar{\sigma}_{13} = 0, \quad (38)$$

subscript  $i = 1, 2$  and  $3$ ; again  $s$ ,  $x_2$  and  $x_3$  are arbitrary,  $s = x_1 - a \ll a$  ( $s > 0$ ) and  $x_2$  is small.  $K_I^0 = \sigma_{22}^a \sqrt{a\pi}$  and  $K_{III}^0 = \sigma_{23}^a \sqrt{a\pi}$  are stress intensity factors for the planar crack in pure modes I and III.  $\bar{\sigma}_{12} = \bar{\sigma}_{13} = 0$  is the value taken by the considered stresses on surface  $x_2 = \xi$ .

#### IV-4. Energy considerations

In the following, an expression for the derivative  $G$  of the energy of the system with respect to crack area is derived. This serves to discuss the initiation of crack motion. We follow Anongba [11] and the procedure is adapted from Bilby and Eshelby [15].

Allow the right-hand front of the non-planar crack with shape (1) (use Fig. 3 to illustrate) to advance (say rigidly for simplicity) from  $x_1 = a$  to  $a + \delta a$ , but apply forces to the freshly formed surfaces to prevent relative displacement; the energy of the system is unaltered. Now allow these forces to relax to zero so that the crack extends effectively from  $a$  to  $a + \delta a$ . The work done by these forces corresponds to a decrease of the energy of the system which we shall estimate (the energy of the system consists of the elastic energy of the medium and the energy of the loading mechanism). The element  $ds = dl dx_1$  ( $l$  runs parallel to the crack front) of the surface  $x_2 = \xi$  (1) ahead of the crack front, at a point  $P = (x_1, x_2 = \xi, x_3)$ , may be defined by  $d\vec{s} = \vec{\gamma} ds$  where  $\vec{\gamma}$  is the unit vector perpendicular to  $ds$  pointing to the positive  $x_2$  direction. We obtain  $d\vec{s} = 1/\sqrt{1 + (\partial \xi / \partial x_3)^2} (0, 1, -\partial \xi / \partial x_3) dx_1 dl$ . The relevant components of the force acting on  $ds$  are  $\bar{\sigma}_{2j} ds_j$  in the  $x_2$  direction and  $\bar{\sigma}_{3j} ds_j$  in the  $x_3$  direction (the summation convention on repeated subscripts applies) where  $\bar{\sigma}_{ij}$  are stresses ahead of the shorter crack; thus the energy change associated with  $ds$  is  $(\bar{\sigma}_{2j} ds_j \Delta u^{(1)} / 2 + \bar{\sigma}_{3j} ds_j \Delta u^{(2)} / 2)$ , where  $\Delta u^{(i)}$  ( $i = 1$  and  $2$ ) are the differences in displacement across the lengthened crack, just behind its tip, in the  $x_2$  and  $x_3$  directions. It becomes now clear that, when the crack advances from  $a$  to  $a + \delta a$ , the energy decrease associated with a surface element  $dl \delta a$  is

$$\begin{aligned}
-\delta E &= \frac{1}{2} \int_a^{a+\delta a} \bar{\sigma}_{2j} ds_j \Delta u^{(1)} + \frac{1}{2} \int_a^{a+\delta a} \bar{\sigma}_{3j} ds_j \Delta u^{(2)} \\
&= \frac{1}{\sqrt{1 + \left( \frac{\partial \xi}{\partial x_3} \right)^2}} \left( \frac{1}{2} \int_a^{a+\delta a} \left( (\bar{\sigma}_{22} - \frac{\partial \xi}{\partial x_3} \bar{\sigma}_{23}) \Delta u^{(1)} + (\bar{\sigma}_{23} - \frac{\partial \xi}{\partial x_3} \bar{\sigma}_{33}) \Delta u^{(2)} \right) dx_1 \right) dl
\end{aligned} \quad . \quad (39)$$

Let  $G$  be the derivative of the energy of the system with respect to crack area.  $G$  corresponds to the limiting value taken by  $-\delta E / dl \delta a$  as  $\delta a$  decreases to zero. Stresses  $\bar{\sigma}_{ij}$  generally consist of terms that are either bounded or unbounded as  $x_1$  tends to  $a$ ; only those stress terms that are singular may contribute a non-zero value to  $G$ ; the bounded terms all contribute nothing.

Using (38) and defining  $\bar{\sigma}^{(i)}(s)$  ( $i=1$  and 2) as

$$\bar{\sigma}^{(i)}(s) \equiv \frac{\delta_{i1} K_I^0 + \delta_{i2} K_{III}^0}{\sqrt{2\pi}} \frac{1}{\sqrt{s}} \quad (40)$$

we arrive at

$$\begin{aligned}
G(P_0) &= \lim_{\delta a \rightarrow 0} -\delta E / dl \delta a \\
&= \frac{1}{\sqrt{1 + (\partial \xi / \partial x_3)^2}} \left( \left[ 1 - \frac{\nu}{1-\nu} M \frac{\partial \xi}{\partial x_3} - \nu \left( \frac{\partial \xi}{\partial x_3} \right)^2 - \frac{1}{2} \left( 1 + \frac{3-\nu}{1-\nu} M \frac{\partial \xi}{\partial x_3} \right) \xi \frac{\partial^2 \xi}{\partial x_3^2} \right] G_0^{(1)} \right. \\
&\quad \left. + \left[ 1 - \frac{\nu}{M} \frac{\partial \xi}{\partial x_3} + \frac{2}{1-\nu} \left( \frac{\partial \xi}{\partial x_3} \right)^2 + \left( \frac{3-\nu}{2(1-\nu)} - \frac{1+\nu}{M} \frac{\partial \xi}{\partial x_3} \right) \xi \frac{\partial^2 \xi}{\partial x_3^2} \right] G_0^{(2)} \right) \quad (41)
\end{aligned}$$

where

$$G_0^{(i)} = \lim_{\delta a \rightarrow 0} \frac{1}{\delta a} \left( \frac{1}{2} \int_a^{a+\delta a} \bar{\sigma}^{(i)} \Delta u^{(i)} dx_1 \right), \quad i=1 \text{ and } 2, \quad (42)$$

and  $M = \sigma_{23}^a / \sigma_{22}^a$ .

Expression (41) gives the value of  $G$  at an arbitrary point  $P_0(a, x_2 = \xi, x_3)$  along the front of the non-planar crack with half length  $a$ . The calculation of  $\Delta u^{(i)}$  depends on the way the extension of the right-hand front of the crack

from  $x_1 = a$  to  $a + \delta a$  is performed. When  $\Delta u^{(i)}$  is obtained from a distribution of dislocations perpendicular to the  $x_1$ -direction, we implicitly assume a rigid crack-front displacement. In that case,  $\Delta u^{(i)}$  may be obtained from the solution of (32) modified to allow for the fact that the crack extends from  $-a$  to  $a + \delta a$  instead of from  $-a$  to  $a$ . Approximate expressions for  $G_0^{(i)}$  ( $i=1$  and 2) correspond to a planar distribution of straight edge and screw dislocations. In that case, Bilby and Eshelby [15] have shown that

$$\begin{aligned} G_0^{(1)} &= K_I^0 (1 - \nu^2) / E \equiv G_0^I, \\ G_0^{(2)} &= K_{III}^0 (1 + \nu) / E \equiv G_0^{III} \end{aligned} \quad (43)$$

where  $E$  is Young's modulus. Adopting approximation (43) and defining  $\tilde{G}(P_0)$  as  $\tilde{G}(P_0) = G(P_0) / (G_0^I + G_0^{III})$ , we obtain

$$\begin{aligned} \tilde{G}(P_0) &= \frac{1}{\sqrt{1 + (\partial \xi / \partial x_3)^2}} \left( 1 - \frac{2\nu M}{1 - \nu + M^2} \frac{\partial \xi}{\partial x_3} + \frac{(3 - \nu)M^2 - (1 - \nu)^2}{2(1 - \nu)(1 - \nu + M^2)} \xi \frac{\partial^2 \xi}{\partial x_3^2} \right. \\ &\quad \left. + \frac{2M^2 - \nu(1 - \nu)^2}{(1 - \nu)(1 - \nu + M^2)} \left( \frac{\partial \xi}{\partial x_3} \right)^2 - \frac{(5 + \nu)M}{2(1 - \nu + M^2)} \xi \frac{\partial \xi}{\partial x_3} \frac{\partial^2 \xi}{\partial x_3^2} \right). \end{aligned} \quad (44)$$

For the planar crack with a straight front, the decrease of the energy of the system ( $-\delta E$ ), divided by the surface element  $dl \delta a$ , is defined as the crack extension force per unit edge length of the crack front (see, for example, Bilby and Eshelby [15]). In the present study, we shall refer to  $G$  (41) as the crack extension force per unit length of the crack front. In Section 4.5 we give a more detailed description of  $G$  for one special crack.

#### IV-5. Segmented crack front

Here the crack front is segmented as illustrated in **Figure 1** and  $B$  is taken as origin.  $\xi$  is then odd and  $(2\lambda = \lambda_A + \lambda_B) -$  periodical with respect to  $x_3$  where  $\lambda_A$  and  $\lambda_B$  (**Figure 1**) are the projected length along  $x_3$  of planar facets with inclination angles  $\phi_A$  and  $\phi_B$  at points  $A$  and  $B$  of the average fracture plane.  $\xi$  is given over a wavelength as

$$\begin{aligned} \xi &= \tan \phi_B x_3, & |x_3| &\leq \lambda_B / 2 \\ &= \tan \phi_A (-x_3 + \lambda), & x_3 &\in [\lambda_B / 2, \lambda_B / 2 + \lambda_A]. \end{aligned} \quad (45)$$

We next consider successively the normalized crack extension force (44),

now denoted  $\tilde{G}_v$ , average  $\langle \tilde{G}_v \rangle = (1/2\lambda) \int_0^{2\lambda} \tilde{G}_v dx_3$  and ultimately the condition for an extremum of  $\langle \tilde{G}_v \rangle$ .

$\tilde{G}_v$  on a period reads

$$\begin{aligned} \tilde{G}_v(P_0) &= \cos \phi_B \left( 1 - \frac{2\nu M}{1-\nu+M^2} \tan \phi_B + \frac{2M^2 - \nu(1-\nu)^2}{(1-\nu)(1-\nu+M^2)} \tan^2 \phi_B \right), \quad |x_3| < \lambda_B / 2 \\ &= \cos \phi_A \left( 1 + \frac{2\nu M \tan \phi_A}{1-\nu+M^2} + \frac{2M^2 - \nu(1-\nu)^2}{(1-\nu)(1-\nu+M^2)} \tan^2 \phi_A \right), \quad x_3 \in [\lambda_B / 2, \lambda_B / 2 + \lambda_A]. \end{aligned} \quad (46)$$

For given  $M$  and crack profile  $(\phi_A, \phi_B)$ , (46) provides the reduced crack extension force at an arbitrary point  $P_0(a, \xi, x_3)$  on the segmented crack front.  $\tilde{G}_v$  takes constant values on facets  $A$  and  $B$ .

$\langle \tilde{G}_v \rangle$  may be written as

$$\langle \tilde{G}_v \rangle = v_0 - v_1 \frac{2\nu M}{1-\nu+M^2} + v_2 \frac{2M^2 - \nu(1-\nu)^2}{(1-\nu)(1-\nu+M^2)} \quad (47)$$

where

$$\begin{aligned} v_0 &= (1/1+\varepsilon)(\cos \phi_A + \varepsilon \cos \phi_B), \\ v_1 &= (1/1+\varepsilon)(-\sin \phi_A + \varepsilon \sin \phi_B), \\ v_2 &= (1/1+\varepsilon) \tan \phi_A (\sin \phi_A + \sin \phi_B) \end{aligned} \quad (48)$$

and  $\varepsilon = \lambda_B / \lambda_A = \tan \phi_A / \tan \phi_B$ .

We restrict ourselves to the condition for an extremum for  $\langle \tilde{G}_v \rangle$  with respect to  $\phi_A$  by cancelling  $\partial \langle \tilde{G}_v \rangle / \partial \phi_A$ . We have from (47)

$$\partial \langle \tilde{G}_v \rangle / \partial \phi_A = v_0 \dot{v} - v_1 \frac{2vM}{1-v+M^2} + v_2 \frac{2M^2 - v(1-v)^2}{(1-v)(1-v+M^2)} \quad (49)$$

where

$$\begin{aligned} v_0 &= \partial v_0 / \partial \phi_A = \partial f_\varepsilon / \partial \phi_A (\cos \phi_A - \cos \phi_B) - f_\varepsilon \sin \phi_A, \\ v_1 &= \partial v_1 / \partial \phi_A = -\partial f_\varepsilon / \partial \phi_A (\sin \phi_A + \sin \phi_B) - f_\varepsilon \cos \phi_A, \\ v_2 &= \partial v_2 / \partial \phi_A = \partial f_\varepsilon / \partial \phi_A \tan \phi_A (\sin \phi_A + \sin \phi_B) \\ &\quad + f_\varepsilon (2 \sin \phi_A + \sin \phi_B - \sin^3 \phi_A) / \cos^2 \phi_A \end{aligned} \quad (50)$$

and

$$f_\varepsilon = 1/1+\varepsilon, \quad \partial f_\varepsilon / \partial \phi_A = -f_\varepsilon^2 / \tan \phi_B \cos^2 \phi_A. \quad (51)$$

$\partial \langle \tilde{G}_v \rangle / \partial \phi_A = 0$  leads to finding the roots of a polynomial of order 2 in  $M$ ; this gives

$$M = (1-v) \frac{v_1 \dot{v} + \sqrt{v^2 v_1^2 + (v_2 \dot{v} - v_0 \dot{v})(1-v)v_0 + 2v_2 \dot{v}}}{(1-v)v_0 + 2v_2}. \quad (52)$$

Equation (52) is the required solution. It leads to positive  $M$  values and agrees with extrema observed on  $\langle \tilde{G}_v \rangle$  as a function of  $\phi_A$ .

**Figures 4, 5 and 6** are plots of  $\tilde{G}_v$  (46),  $\langle \tilde{G}_v \rangle$  (47) and points  $(\phi_A, M)$  (52) for  $\phi_B = \text{constant}$ . For a given  $\phi_B$ , one can distinguish different behaviours as a function of  $M$ . This description applies to any  $\phi_B$ . Consider  $\phi_B = \pi/2.57 = 70^\circ$  to illustrate. **Figure 6** gives  $M$  in the interval  $[0.3022, 0.3992]$ . First  $M$  increases with  $\phi_A$  from  $0.3022$  ( $\phi_A = 0$ ) to  $0.3992$  ( $\phi_A \approx 40^\circ$ ); these  $(\phi_A, M)$  correspond to a maximum larger than 1 for  $\langle \tilde{G}_v \rangle$  when plotted against  $\phi_A$ ; this is the case for the pair  $(\phi_A = 21.15^\circ, M = 0.38)$ , **Figure 5**. Then, from maximum  $M = 0.3992$  ( $\phi_A \approx 40^\circ$ ), **Figure 6**,  $M$  decreases with  $\phi_A$ ; these  $(\phi_A, M)$  correspond to a minimum for  $\langle \tilde{G}_v \rangle$ ; this is the case for the point  $(\phi_A = 59.10^\circ, M = 0.38)$ , **Figure 5**. Outside  $[0.3022, 0.3992]$ ,  $\langle \tilde{G}_v \rangle$  decreases continuously with  $\phi_A$  for  $M < 0.3022$  ( $M = 0.3$ , **Figure 5**, for instance) and increases indefinitely with  $\phi_A$  for  $M > 0.3992$  ( $M = 0.5$ ,

**Figure 5**): in the latter situation there is no maximum. **Figure 4** shows  $\tilde{G}_v$  along the crack front for three different  $M$  (0.3, 0.38 and 0.5) corresponding to values located below, inside and above [0.3022, 0.3992] with  $\phi_A = \pi/7.85 \cong 23^\circ$  and  $\phi_B = \pi/2.57 \cong 70^\circ$ .  $\tilde{G}_v$  takes constant different values, given by Equation (46), in  $x_3$  – interval  $]-\lambda_B/2, \lambda_B/2[$  and  $]\lambda_B/2, \lambda_B/2 + \lambda_A[$  and increases with  $M$ , **Figure 4**.

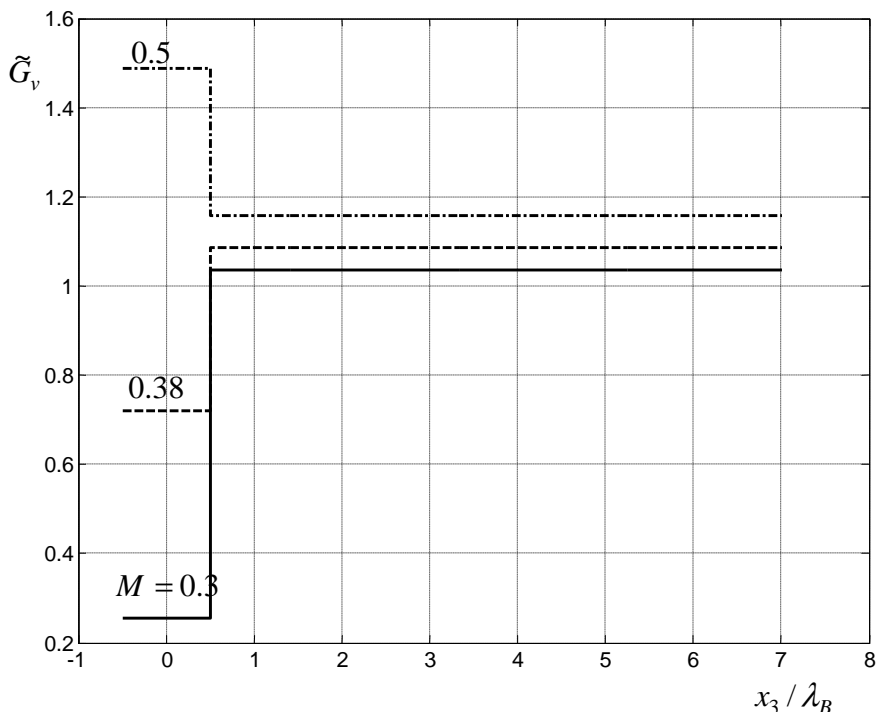


**Figure 4** : Normalized crack extension force  $\tilde{G}_v$  (46) for the segmented crack front as a function of  $x_3$  (reduced by  $\lambda_B$  defined in **Figure 1**). The curves correspond to  $M = 0.3$ , 0.38 and 0.5; they take different constant values in intervals  $]-1/2, 1/2[$  and  $]1/2, 1/2 + 1/\varepsilon[$  where  $\varepsilon = \lambda_B / \lambda_A = \tan \phi_A / \tan \phi_B$ ,  $\phi_A = \pi/7.85$ ,  $\phi_B = \pi/2.57$  and  $\nu = 1/3$ .

In summary, for a given  $\phi_B$  there exists a value  $M$ , say  $M_t$  (given by (52) when  $\phi_A = 0$ ), such that:

- When  $M > M_t$  there are  $\phi_A$  values limited by zero (as discussed above) corresponding to  $\langle \tilde{G}_v \rangle > 1$ ; under such conditions non-planar crack motion is possible. A local maximum is observed in the  $\langle \tilde{G}_v \rangle$  dependence on  $\phi_A$  only for moderate  $M$  (**Figure 5**).
- When  $M \leq M_t$ ,  $\langle \tilde{G}_v \rangle \leq 1$  for any  $\phi_A$ ; non-planar crack propagation is unexpected.

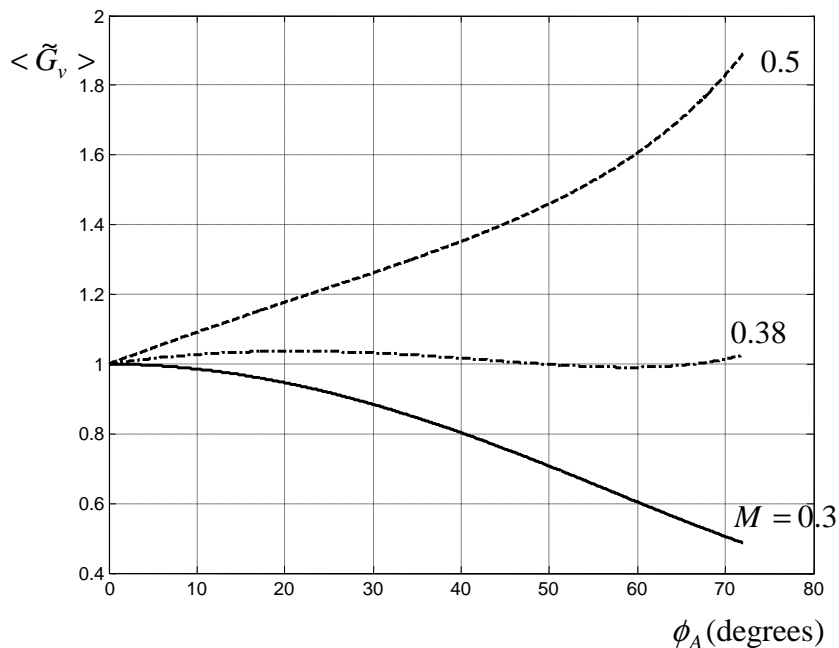


**Figure 5** : Reduced crack extension force averaged over  $x_3$ ,  $\langle \tilde{G}_v \rangle$  (47), as a function of the inclination angle  $\phi_A$  of crack-front segment A;  $\phi_B = \pi/2.57 \cong 70^\circ$ ;  $\nu = 1/3$ .  $M = 0.3$  : the corresponding curve decreases continuously as  $\phi_A$  increases.  $M = 0.38$  : the associated curve displays a local maximum (above 1) and a local minimum (below 1) at  $\phi_A$  values given by (52) (see also **Figure 6**, curve  $\pi/2.57$ ).  $M = 0.5$  : the corresponding curve increases continuously with  $\phi_A$ .

## V - DISCUSSION

### V-1. On the hypotheses and method of analysis in the present study

Expressions for the displacement and stress fields of a dislocation of edge average character (Section 2) are established from a linear form with respect to  $\xi$  (2) of plastic distortion  $\beta_{12}^*$  (note that the exact relation is  $\beta_{12}^*(\vec{x}) = b\delta(x_1)H(x_2 - \xi)$ ). Relation (2) is valid under the condition  $\xi$  small only, the shape of  $\xi$  being arbitrary, with the meaning that there is no restriction on its spatial derivatives ( $\partial\xi/\partial x_3$  and  $\partial^2\xi/\partial x_3^2$ , particularly). No additional hypothesis is introduced (see Section 2) indicating that displacement and stress fields (14) and (16) are also valid under  $\xi$  small only. This condition applies to corresponding elastic fields of a dislocation of screw average character (Section 3) since same linear form with respect to  $\xi$  (18) of plastic distortion  $\beta_{13}^*$  is used.

From stresses due to dislocations, we obtain successively stresses  $\bar{\sigma}_{ij}$  (38) about the crack front and crack extension force  $G$  (41) per unit length of the crack front. The calculation of these quantities involves integrals (see (42) for example) that are executed approximately by using elastic fields due to a planar distribution of straight dislocations. However these additional hypotheses have no direct influence on the geometrical factors (i.e. those with  $\xi$  and its spatial derivatives  $\partial\xi/\partial x_3$  and  $\partial^2\xi/\partial x_3^2$ ) present in results (38), (41) and (44). In short, the results of the present study are obtained under the condition  $\xi$  small only. There is no restriction on the spatial derivatives of  $\xi$ .

The traction free boundary condition at an arbitrary point  $P(x_1, x_2 = \xi, x_3)$ ,  $|x_1| < a$ , of the faces of the crack reads

$$\bar{\sigma}_{ij}\gamma_j = 0 \quad (53)$$

where  $\bar{\sigma}_{ij}$  and  $\gamma_j$  are total stress and component  $j$  of unit vector normal to the crack face at  $P$  respectively. We show below that our analysis in Section 4 correctly reproduces (53). More precisely we shall show that Equation (53) is

equivalent to (25) when  $i=2$  and to (26) when  $i=3$ . Equation (53) gives, when  $i=2$ ,

$$\bar{\sigma}_{22} + \bar{\sigma}_{23}\gamma_3/\gamma_2 = 0. \quad (54)$$

$\bar{\gamma} = 1/\sqrt{1 + (\partial\xi/\partial x_3)^2}$   $(0,1, -\partial\xi/\partial x_3)$  (see Section 4.4);  $\bar{\sigma}_{ij}$  is given by Equations (36) and (37):

$$\begin{aligned} \bar{\sigma}_{22} &= \sigma_{22}^a + \int_{-a}^a \sigma_{22}^{(1)} D_1 dx_1 + \int_{-a}^a \sigma_{22}^{(2)} D_2 dx_1, \\ \bar{\sigma}_{23} &= \sigma_{23}^a + \int_{-a}^a \sigma_{23}^{(1)} D_1 dx_1 + \int_{-a}^a \sigma_{23}^{(2)} D_2 dx_1. \end{aligned}$$

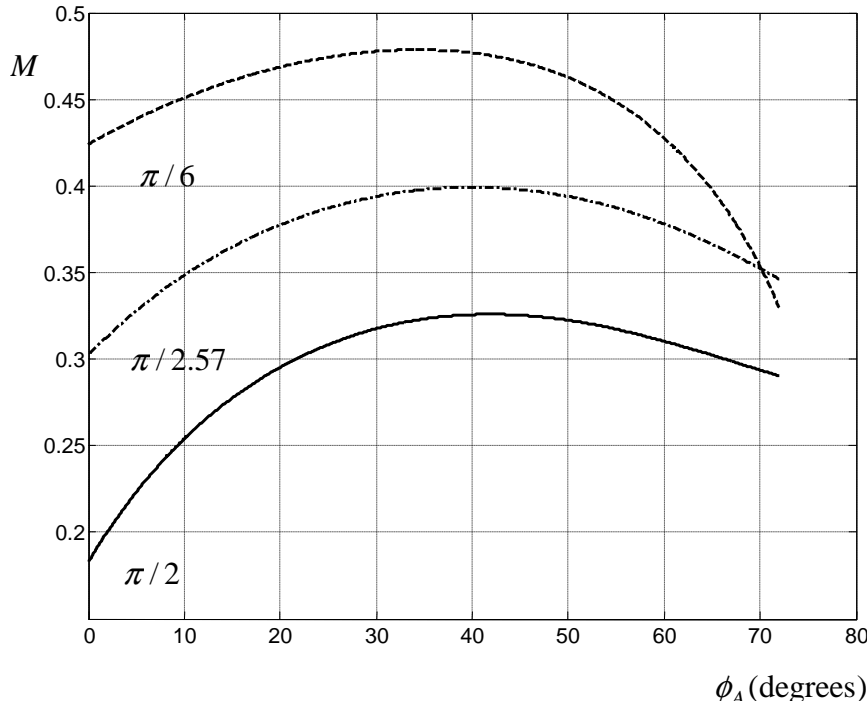


**Figure 6 :** Points  $(\phi_A, M)$  ( $\phi_B = \text{constant}$ , Equation (52)) for which  $\langle \tilde{G}_v \rangle$  (47)

is extremum when plotted against  $\phi_A$  as in **Figure 5** with  $M = 0.38$  ;  $\nu = 1/3$  ; segmented crack front. The curves correspond to  $\phi_B = \pi/2$ ,  $\pi/2.57$  and  $\pi/6$  : in any of these curves, points before (from the left) the maximum correspond to  $\langle \tilde{G}_v \rangle$  maximum and larger than 1 and points after the maximum to  $\langle \tilde{G}_v \rangle$  minimum and smaller than 1.

Introducing above expressions in (54) and noting that  $\partial\xi/\partial x_3 = -\gamma_3/\gamma_2 = t_2/t_3$  (for  $t_j$  see Section 4.1) we recover Equation (25). Similarly (53) yields (26) when  $i=3$ . Equations (25) and (26) (summarized into (27)) are governing integral equations (they contain externally applied stresses  $\sigma_{22}^a$  and  $\sigma_{23}^a$ ) that provide equilibrium dislocation distributions  $D_1$  and  $D_2$ . In Section 4.2, a procedure to solve (27) has been proposed and approximate solutions (34) for  $D_1$  and  $D_2$  given. One further step is to confront our analysis with experiments in order to check on the validity of the present modelling (see below).

## V-2. Comparison with previous theoretical analyses and experiments

One may distinguish (arbitrarily) two types of studies involving the non-planar character of loaded cracks. On the one hand, there are works providing formulae for elastic quantities (stress, stress intensity factors, displacement...) about the front of a crack that is entirely non-planar, as the present study does: Gao [6], Xu et al. [7], Ball and Larralde [9], Anongba [11], Movchan et al. [8], among others. On the other hand, there are works interested in elastic quantities about the front of an initially planar crack that adopts over a short distance of further propagation a non-planar configuration: the recent work of Lazarus et al. [10] for instance.

Consider first type of studies by Gao [6], Xu et al. [7], Movchan et al. [8] and Ball and Larralde [9]. These authors have considered an infinite solid with a non-planar crack whose surface  $\xi = \xi(x_1, x_3)$  (in our notation) depends on both  $x_1$  and  $x_3$  and may be viewed as a slight perturbation of a planar semi-infinite straight edge crack; we stress that in the work by Ball and Larralde [9],  $\xi = \xi(x_3)$  depends on  $x_3$  only. In all these studies both  $\xi$  and its spatial derivatives  $\partial\xi/\partial x_1$  and  $\partial\xi/\partial x_3$  are taken small and linear expressions of SIF are given. These results have a narrow application. Actually these apply to a crack that propagates essentially under mode I loading but whose front, for various possible reasons, suffers a slight perturbation. Indeed, when a mode II loading (in addition to mode I) is applied to a planar crack located in  $x_1 x_3$ , the subsequent fracture propagation path departs from  $x_1 x_3$  (Erdogan and Sih [18], Radon et al. [19]) and condition  $\xi$  small is violated; for applied mode III and as mentioned earlier in Section 1,  $\xi$  is generally small but  $\partial\xi/\partial x_3$  measured in the crack front  $x_3$  direction may be large (on facets  $B$  for instance, **Figure 1**) even under  $M$  small.

Let us assume (as in these earlier works) both  $\xi$  and its spatial derivatives to be small. Under such conditions only linear terms in the reduced crack extension force (44) are considered to survive and we may write

$$\tilde{G}(P_0) \approx 1 - \frac{2\nu M}{1-\nu+M^2} \frac{\partial \xi}{\partial x_3}. \quad (55)$$

In Section 4.5, we have performed an average  $\langle \tilde{G} \rangle$  of  $\tilde{G}$  using (44). The same procedure using (55) reduces the result to that of the planar crack when the crack front has a segmented front (Section 4.5); since it is assumed that  $\partial \xi / \partial x_3$  is small, this means that  $\tan \phi_A \approx \phi_A$  and  $\tan \phi_B \approx \phi_B$ ; because  $\phi_A$  and  $\phi_B$  have similar small magnitude,  $\langle \tilde{G} \rangle$  using (55) is virtually one. Hence to discuss macroscopic crack properties, it is necessary to use more elaborate expressions such as (44) valid under condition  $\xi$  small only (see Section 5.1). One may justly be interested in a detailed comparison between stress or SIF formulae obtained in the present study and those derived in earlier works (Gao [6]; Xu et al. [7]; Movchan et al. [8]; Ball and Larralde [9]). Actually such a comparison is not straightforward because our crack geometry (Section 4.1) is very different from the one (mentioned above) adopted in these previous studies. Therefore our results are expected to be different from theirs. Furthermore we have obtained formulae for the stress about the crack front from the stress fields due to dislocations whereas earlier works used perturbation methods associated with brittle fracture mechanics. This leads to different definitions and presentations of results. However a general comparison can briefly be made along the following lines. Firstly we note that stresses  $\bar{\sigma}_{12}$  and  $\bar{\sigma}_{13}$  (38) are zero on our crack front leading to  $K_{II} = 0$ . Our crack model predicts that there is no coupling between modes I and II on the one hand and modes III and II on the other to linear order in  $\xi$ . The non existence of coupling between modes III and II can also be reached in the perturbation analysis of plane cracks by Gao [6] that makes use of crack-face weight functions. Assuming the crack faces to be traction free (relation (10) of Gao [6]), the  $K_{II}$  expression (see (13) in Gao [6] for example) involves terms with stresses (in our notation)  $\bar{\sigma}_{13}^0$ ,  $\bar{\sigma}_{33}^0$  and  $\bar{\sigma}_{11}^0$  produced in the surrounding medium by a planar crack as well as their first derivatives with respect to  $x_1$  and  $x_3$ . In our crack geometry (planar crack in  $x_1 x_3$  extending from  $x_1 = -a$  to  $a$ ), it is easy to see (use (36)(37) applied to the planar crack and (22)(17) for instance) that all these quantities and associated derivatives

cancel on the  $x_1x_3$  – plane in pure mode III, leading to  $K_{II} = 0$ . Turning to a different crack geometry, we observe that for the planar semi-infinite crack with a straight edge front,  $\bar{\sigma}_{12} = \bar{\sigma}_{13} = 0$  (in our notation) at the crack tip on the fracture plane in pure modes I and III (see the so called Irwin near-field solutions displayed by Lawn [5]). When the crack is non-planar semi-infinite,  $K_{II}$  takes a non-zero value (see (36) in Ball and Larralde [9] and (3.40) in Movchan et al. [8]). The discrepancy as compared to our result above may originate essentially from a difference in crack geometries under mode I loading. Secondly under pure mode I and III loadings, the  $K_{III}$  and  $K_I$  induced by the shape of the non-planar crack are (to first order)  $(1-\nu)\partial\xi/\partial x_3 K_I^0$  and  $(1/\nu-1)\partial\xi/\partial x_3 K_{III}^0$  respectively (in conformity with (55)). These agree in form with corresponding results presented by Ball and Larralde [9] (see their relations (36) and (37)) and Movchan et al. [8] (see their (3.40)); by “agree in form” we mean that results given by these authors are proportional to the derivative  $\partial\xi/\partial x_3$  of the perturbation as in the present work. We want to stress here that Lazarus et al. [10], in a similar comparison, have found agreement between some of their results (their relation (52)) and previous results of Ball and Larralde [9] (their (36)) and Movchan et al. [8] (their (3.40)).

We turn to Lazarus et al. [10] which consider an initially planar semi-infinite straight edge crack (crack front in the  $x_3$ -direction) that adopts a non-planar configuration after fracture propagation over a short distance  $\delta$  (in their notation), the new crack surface  $\xi = \xi(x_3, \delta)$  (in our notation) being  $x_3$  and  $\delta$  dependent. The only small parameter is  $\delta$  (or equivalently  $\xi$ ); there is no restriction on the spatial derivatives of  $\xi$  (as in the present study). A question that can be posed is: under which conditions can the approach of these authors be used to express the stress fields about the front of a macroscopic crack entirely non-planar? It appears evident that it is necessary that  $\delta$  be sufficiently large. They provide stress intensity factors to first order in  $\delta$  and use the usual plane strain relation to estimate the crack extension force  $G$ .

We now compare our analysis with experiments and first focus on the situation where the average value of the reduced crack extension force is larger than 1 and the crack-front inclination angle  $\phi_A$  takes moderate values (i.e. ranging from zero to  $50^\circ$  approximately). From Section 4, it is seen that this occurs when  $M \geq 0.183$  for  $\phi_B = \pi/2$  and  $M \geq 0.302$  for  $\phi_B = \pi/2.57$ , **Figures 5 and 6**, for example. Assuming that crack motion may occur when

the average value of the normalized crack extension force is larger than 1, our analysis suggests that non-planar cracks with segmented front with  $\phi_B \approx \pi/2$  are favoured at small  $M$ . This is in full agreement with experiments (Sommer [1]; Cooke and Pollard [2]).

We also mention an apparently interesting property of the model. Consider a crack with segmented front and take  $\phi_B = \pi/2.57$  to illustrate **Figure 5**; we have indicated in Section 4.5 that for  $M$  sufficiently large ( $M \geq 0.4$ ), the average  $\langle \tilde{G}_v \rangle$  increases continuously with  $\phi_A$  from the value 1 ( $\phi_A = 0$ ). This suggests that  $\phi_A$  may increase gradually as the crack extends. However it is clear that the crack model of the present study, by construction, is unable to describe quantitatively any change of  $\phi_A$  with crack length as depicted by Sommer [1] for instance.

Several theoretical criteria have been proposed in an attempt to explain the dependence of  $\phi_A$  on the ratio  $M$  of the applied stresses [2]: these are based on the crack-tip stress field of a planar crack subjected to mixed mode I+III loading. They all lead to the same equation (56) for moderate  $M$  [2, 20]; a simple explanation is that incipient cracks grow from the parent crack front at twist angle  $\phi_A$ , from the original crack plane, for which they suffer no shear stresses;

$$\phi_A = \frac{1}{2} \tan^{-1} \left( \frac{M}{1/2 - \nu} \right) \quad (56)$$

Predicted angles of twist depend on Poisson's ratio  $\nu$  and vary from 0 to  $45^\circ$  for  $M$  ranging from 0 to infinity. Unfortunately, as can be seen from **Figure 2**, measured angles fall markedly below theoretical prediction (56). We have also plotted on **Figure 2** the points  $(\phi_A, M)$  ( $\phi_B = \text{constant}$ , Equation (52)) for which  $\langle \tilde{G}_v \rangle$  (47) is maximum and larger than 1: curve (2) corresponds to  $\phi_B = \pi/2$  and curve (3) to  $\phi_B = \pi/4$ . These additional curves, provided by the present study, fall inside experimental points for moderate  $M$  ( $M \leq 0.5$ , approximately). For larger  $M$  values, as mentioned earlier (Section 4.5), there is no local maximum on  $\langle \tilde{G}_v \rangle$  when plotted against  $\phi_A$  ( $M = 0.5$  in **Figure 5** for example) and a different criterion is required. It is important to mention that, for the experimental points given in **Figure 2**, we have no information about corresponding  $\phi_B$ . A detailed comparison with experiments, with the aim of improving existing models, should take full account of the whole observed shape of the crack front.

## VI - CONCLUDING REMARKS

- A model of non-planar crack of finite length under mixed mode I+III loading, fluctuating about an average fracture  $x_1x_3$  – plane, has been investigated. The crack front has an arbitrary periodical shape  $\xi(x_3)$  spreading in a plane perpendicular to the crack propagation  $x_1$  – direction. We have established expressions for both the stress about the crack front (38) and the crack extension force  $G$  per unit length of the crack front (41) (44). We have averaged  $G$  over  $x_3$  for one special crack with a segmented front and established conditions linking applied stress to crack-front profile under which the average crack extension force  $\langle G \rangle$  is maximum and larger than the value corresponding to that of the planar crack under mixed mode I+III. These conditions conform to experimental situations in which non-planar cracks are favourably observed.
- The crack is macroscopic in our modelling (Section 4.1) since it runs indefinitely in the  $x_3$  – direction. This is a well-formed crack with length  $2a$  roughly of the order of 1 mm in ordinary laboratory experiments. In the  $x_1x_2$  – plane, the crack is surrounded by an infinite medium under mixed mode I+III with loadings applied at infinity. In this geometry, there is apparently no reason for the non-planar crack to depend on  $x_1$ . Thus the reduced crack extension force (44) remains practically unchanged when in addition one assumes the crack front to depend on crack length. This is because the additional stresses that come into play in the calculation of the crack extension force,  $\bar{\sigma}_{12}$  and  $\bar{\sigma}_{13}$  (38), are zero in both cases (crack front being only  $x_3$  or both  $x_1$  and  $x_3$  dependent); also the other stresses  $\bar{\sigma}_{22}$  and  $\bar{\sigma}_{23}$  (38) remain unchanged in form. Only when applied mode II loading (in addition) is assumed on our crack model will the crack length play a clear role in the fracture properties of the cracked solid.
- The present modelling assumes the shape  $\xi$  of the crack front to be independent of crack length. It may be argued that this is a serious limitation. However the present work deserves consideration for a number of reasons. First the method used to give expressions for the stress about the non-planar crack front and crack extension force is different from those available in the literature; it makes use of explicit expressions of dislocation (say, sinusoidal edge or screw dislocation (Anongba [12]) stress fields. Furthermore we claim that this method

of analysis is powerful when applied to the general loading (mode I+II+III) of a non-planar crack with inclined (with respect to the applied tension direction) average fracture surface. This problem requires that  $\xi$  be both  $x_1$  and  $x_3$  dependent.

## REFERENCES

- [1] - E. SOMMER, *Eng. Fract. Mecha.*, 1 (1969) 539 - 546
- [2] - M.L. COOKE and D.D. POLLARD, *J. Geophys. Res.*, 101 (1996) 3387 - 3400
- [3] - J.R. YATES and K.J. MILLER, *Fatigue Fract. Eng. Mater. Struct.*, 12 (1989) 259 - 270
- [4] - F. HOURLIER and A. PINEAU, *Mém. Sci. Rev. Métall.*, 76 (1979) 175 - 185
- [5] - B.R. LAWN, “Fracture of brittle solids”, Ed. Cambridge University Press, Cambridge (1993)
- [6] - H. GAO, *ASME J. Appl. Mech.*, 59 (1992) 335 - 343
- [7] - G. XU, A.F. BOWER and M. ORTIZ, *Int. J. Solids Struct.*, 31 (1994) 2167 – 2193
- [8] - A.B. MOVCHAN, H. GAO and J.R. WILLIS, *Int. J. Solids Struct.*, 35 (1998) 3419 - 3453
- [9] - R.C. BALL and H. LARRALDE, *Int. J. Fract.*, 71 (1995) 365 - 377
- [10] - V. LAZARUS, J.-B. LEBLOND and S.-E. MOUCHRIF, *J. Mech. Phys. Sol.*, 49 (2001) 1399 – 1420, *Ibid.*, 1421 - 1443
- [11] - P.N.B. ANONGBA, *Physica Stat. Sol. B*, 194 (1996) 443 - 452
- [12] - P.N.B. ANONGBA, *Physica Stat. Sol. B*, 190 (1995) 135 - 149
- [13] - T. MURA, “Micromechanics of defects in solids”, Ed. Martinus Nijhoff Publishers, Dordrecht (1987)
- [14] - B.A. BILBY, A.H. COTTRELL and K.H. SWINDEN, *Proc. Roy. Soc. A*, 272 (1963) 304 – 314
- [15] - B.A. BILBY and J.D. ESHELBY, In: “Fracture”, Ed. Academic Press (H. Liebowitz), New York, Vol 1 (1968) 99 - 182
- [16] - M.O. PEACH and J.S. KOEHLER, *Phys. Rev.*, 80 (1950) 436 – 439
- [17] - P.N.B. ANONGBA and V. VITEK, *Int. J. Fract.*, 124 (2003) 1 - 15
- [18] - F. ERDOGAN and G.C. SIH, *Trans. Am. Soc. Mech. Engng.*, 85 (1963) 519 – 527
- [19] - C.C. RADON, P.S. LEVER and L.E. CULVER, In: “Fracture”, Ed. UW Press, Vol 3 (1977) 1113 – 1118
- [20] - D.D. POLLARD, P. SEGALL and P.T. DELANEY, *Geol. Soc. Am. Bull.*, 93 (1982) 1291 - 1303